URBAN'S RIVER FLOOD ANALYSING USING SENTINEL-1 DATA CASE STUDY: (GORGANROOD, AQ'QALA)

K. Ganji [1*], S. Gharachelou [2], A. Ahmadi [3]

[1] M-Sc. Student, Civil Engineering Faculty, Shahrood University of Technology, Iran - kamranganji@shahroodut.ac.ir
[2] Civil Engineering Faculty, Shahrood University of Technology, Iran - sgharachelo@shahroodut.ac.ir
[3] Civil Engineering Faculty, Shahrood University of Technology, Iran - a.ahmadi@shahroodut.ac.ir

KEY WORDS: ANALYSING, AQ'QALA, FLOOD, SAR, SENTINEL-1, GORGANROOD.

ABSTRACT:

Flood is one of the greatest disasters in the world, and the cause of a lot of damages to buildings and Agricultural products every year. Gorganrood river crossing the city of Aq'qala and it is always under flood risk. In the spring, due to the high intensity rainfall and melting of the snow, upstream areas bring much water into the Gorganrood river. On 23rd March, 2019 occurred a terrible flood in Aq'qala passing discharge 650 (m^3 /s), it would occur every 100 years in this river. This river in normal time is passing discharge approximately 120 (M^3 /S). A large of an urban and non-urban area was affected by this flood and mapping and analyzing of this flood have a key role for river and disaster management. Remote sensing is one of the best ways to flood mapping, especially in flood time weather is cloudy, Therefore, Synthetic Aperture Radar (SAR) images had high potentiality for flood analysis. In this study the Sentinel-1 data used for flood studying due to free available and shorter revisit time. After the processing has done, by selecting the VV band the flooded areas detected. After that overlapped the images and combination of RGB bands and the change the value of pixels, at last, we will be able to obtain the flood mapping images for Gorganrood river. In the primary days of the flooding, almost all the northern regions of the city were flooded, and during a week about 96.8 (KM^2) city flooded.

1. INTRODUCTION

Flooding affects societies, economies, and ecosystems worldwide and can have devastating impacts. For the development of flood risk mitigation plans or disaster relief services, information about the flood extent in affected regions is an important information source for many institutions involved in crisis management, such as relief organizations, governmental authorities, and insurance companies (De Moel et al., 2009a). For effective response during flooding events, the rapid monitoring of flood situations, including mapping the extent of the inundation and damage, is highly critical (Amarnath and Rajah, 2016a; Chowdhury and Hassan, 2017a). Before any flood event, flood forecasting and simulation of the inundation extent is critical for risk mitigation (Shen et al., 2019a).Satellite remote sensing data, especially Synthetic Aperture Radar (SAR), allows one to overcome these challenges and covers an extensive area of the Earth's surface for a near real time detection of large-scale flood events independent of daylight and weather conditions (Betbeder et al., 2013a; Klemas, 2013a).

Flood is one of the most common disasters in the Golestan province, especially in the northern cities of the province, because there is no suitable condition for collecting floodwater. In Golestan province, floods often occur when the sky is covered by clouds, thus making the utilization of optical satellite images is infeasible in providing inundation mapping during the disaster. Therefore, space borne synthetic aperture radar (SAR) systems are the most preferred option for monitoring the flood condition. There are several small rivers in that area, the biggest river is Gorganrood that crossing in many cities such as Aq'qala, Siminshahr, Gonbadkavoos, Bandartorkman, sea, dam, or swamp. Gorganrood river has been changing over the past time, such as morphology aspect, exceeded to the river buffer zone, removing uncontaminated sand and gravel from their beds, building inappropriate bridges on rivers, or dredging them. This has a river in spring and summer due to downpour rain and melts snow passes more discharge about 300 (m^3 /s). On 23rd March 2019 has occurred a terrible flood that discharge was 650 (m^3 /s) and whole Aq'qala city was flooded. Synthetic Aperture Radar (SAR) is the best choice for identify flooded area. The aim of this research is the time series flood mapping using Sentinel-1 data and analyzing with urban river characteristics.

2. STUDY AREA AND DATA REQUIRMENTS

2.1 Study Area

The city of Aq'qala is in Golestan province, that was located in geographical coordinates of 37.00'46" to 37.00'53" North and 54.26'04" to 54.29'20" East. The Aq'qala city is located across the Gorganrood river and the north of Gorgan city. From the north it is confined to Atrak, from the west to the central part of Bandar Turkmen and Gomishan, from the south to the central part of Gorgan and Malek village, and to the east it is confined to Katul district and the central part of Gonbadkavoos city.

Gorganrood River is one of the most important tributaries of Golestan province. The river, with a length of about 300 KM, with a catchment area of 10250 (KM^2), which originates from the northern slopes of eastern Alborz and the western slopes of the northern Khorasan highlands. The river flows from east to west and its tributaries originate from the Alborz Mountains and flow from south to north. Passing through the cities of

* Corresponding Author

https://doi.org/10.5194/isprs-archives-XLII-4-W18-415-2019

Gonbadkavoos and Aq'qala in the west, Khajehenafas into the Caspian Sea by forming a large delta. The average annual discharge Gorganrood river is about 920 million cubic meters. District of Aq'qala city and Gorganrood river shown in Fig. 1.

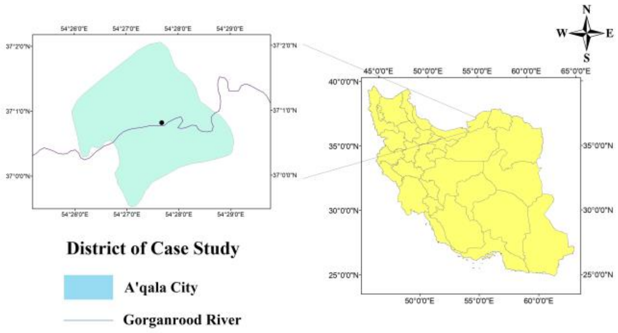

Figure 1. District of Aq'qala city and Gorganrood river

2.2 Sentinel-1 Data

The Sentinel-1 mission consists of two satellites (Sentinel-1A/B) equipped by C-band (wavelengths [λ] = 5.6 cm) sensors that allow one to monitor the Earth's surface at a repeat frequency of six days (Tsyganskaya et al., 2018a).

For flood mapping is used the Sentinel-1 SAR data. Firstly, five scenes Sentinel-1 data downloaded from Sentinel-1 data hub. One scene was before flooded events, and three scenes are on flooding time, and another scene is after the flood. Properties of the scenes have been described in Table 1.

Data	Mission Date	Pass
S1A-IW-GRDH-1SDV-T022830	MAR-11-2019 02:27:23.44	Descending
S1A-IW-GRDH-1SDV-T022830	MAR-23-2019 02:27:23.62	Descending
S1A-IW-GRDH-1SDV-T141953	MAR-29-2019 14:18:48.18	Ascending
S1A-IW-GRDH-1SDV-T022831	APR-04-2019 02:27:23.90	Descending
S1A-IW-GRDH-1SDV-T022831	APR-16-2019 05:17:32.19	Descending

Table 1. Sentinel-1 data used for the study area

Raw satellite images were downloaded, required to pre-processing such as Atmospheric correction, Calibration, Radiometric correction, Thermal noise removal, Terrain correction. We used (SNAP V.6) for applying this pre-processing.

3. PROPOSED METHOD

3.1 Image Pre-Processing

In this study, the Sentinel-1A IW GRD products of VV and VH polarizations have been processed using Sentinel Application Platform (SNAP) tool. The pre-processing steps using SNAP tool are given in Fig. 2. The standard procedures such as orbit correction, thermal noise removal, calibration sigma0, speckle filtering and terrain correction have been applied on the raw SAR images to obtain the geometrically correct image along with backscattering values sigma0 (Clement et al., 2017a; Twele et al., 2016a). A 7*7 Gamma MAP filtering method has been used for speckle suppression of the Sentinel-1A GRD SAR images. The sigma0 values have been converted into a logarithmic scale, i.e. decibel (dB).

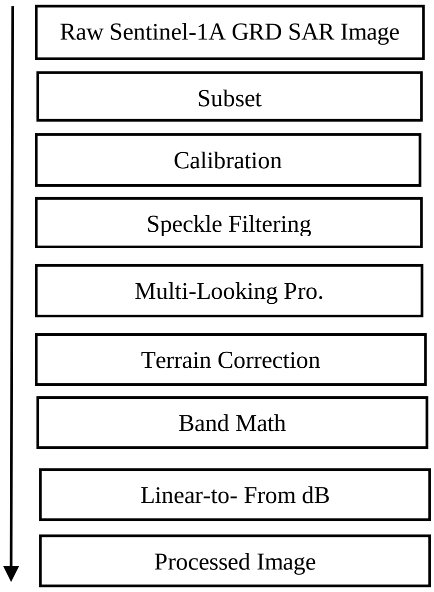

Figure 2. Pre-processing Steps of Sentinel-1A GRD SAR Image

Many researchers concluded that the VV polarization of Sentinel-1A IW GRD product is appropriate for flood detection (Twele et al., 2016a). But VV polarization is more affected by wind-induced ripples on the surface of the floodwaters than other polarizations (Manjusree et al., 2012a).

During the Sentinel-1 pre-processing, Level-1 images were imported into the SNAP Desktop tool. all processing steps were assembled and connected through Graph Builder, which described step by step in continue:

a. To begin pre-processing, scene of Aq'qala city was separated using subset command.
b. Radiometrically corrected by applying annotated image calibration constants to arrive at physically meaningful radar backscatter pixel values, by calibrating the image, the maximum and minimum pixel values are 57.88 and 0.002, respectively.
c. speckle filters were applied to reduce the granular noise characteristic to SAR data.
d. multi-look processing was carried out to reduce the speckle further and improve image interpretability, we used three for Number of Range Looks and Number of Azimuth Looks and Mean GR square Pixel was 30.
e. Terrain Correction present in the SAR images were corrected by transforming the coordinates to a standard reference frame. The standard references were used for distortion correction were, SRTM 3Sec for Digital Elevation Model and BILINEAR-INTERPOLATION for DEM and Image Resampling Method and then WGS84(DD) for Map Projection.
f. In Band Math select the Sigma0_vv_db band, due to the histogram select 16 which it is the boundary between water and land, which is obtained by increasing or decreasing the upper and lower limits of the pixel reflectance. Type this command in Band Math for identify the flooded area: (if sigma0_vv_db < -16 then 1 else NaN). values of less than -16 dB

flooded area are white and values of greater than -16 dB non-flooded area are black.

g. Finally, a radiometric conversion from a linear scale to a dB scale was conducted using the following expressions:

$$\sigma^0_{dB} = 10\log_{10}\sigma^0 \qquad (1)$$

where, σ^0_{dB} backscattering image in dB, σ^0 Sigma bad image. The pre-processed images were exported for image classification.

3.2 Image Classification

The RGB clustering is the most common technique for data compression and iso-clustering works better on an optimal number of classes usually unknown (Mohamed and Verstraeten, 2012a). The RGB clustering functions are a simple classification algorithm that quickly compresses a three-band image into a single-band pseudo-color image without necessarily classifying any particular features and without a signature file and decision rule. The RGB clustering provides greater control over the parameters used to partition the pixels into similar classes (Kumar et al., 2016a). For clustering in this research, we used Create Stack for overlaying the images, Sigma0_VV_11March2019 and Sigma0_VV_23March2019 bands were selected, before flooding and after flooding, respectively. Then by changing the pixel values, the black and white values in the images change, by adjusting it to a suitable state, the identification of the flooded and non-flooded areas is well represented. The value of pixels for before and after flooding were, -17.56, -10.42, -3.28, min, mean, max, respectively. Finally, after the pixel values have been determined, we used the Layer Manager command for RGB clustering. Select the Sigma0_VV_db_slv2_11Mar2019 for RED channel and Sigma0_VV_db_mst_23March2019 for GREEN channel and Sigma0_VV_db_23Mar2019 for BLUE channel. To combine the bands, we select the red band that is the image before the flood and the green and blue bands are the image after the flood to show the dry areas in blue or green or a combination of them. Combination of RGB clustering shown in Fig. 3.

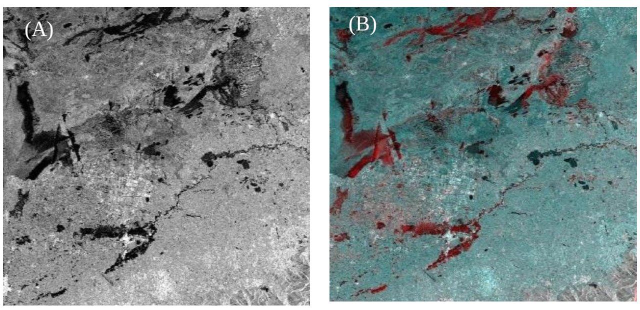

Figure 3. (A) HSV Image Cluster, (B) RGB Image Cluster

3.3 Reflectance Analysis

After radiometric and geometric processing and conversion of bands from Linear to dB, band analysis revealed that in all images after histogram analysis, the interval between the reflection of non-flood points was approximately -16 dB. By specifying it in Band math and converting it into a fuzzy band that represents flood zones of non-floods. The reflectance of pixels for time series are shown in Fig.4.

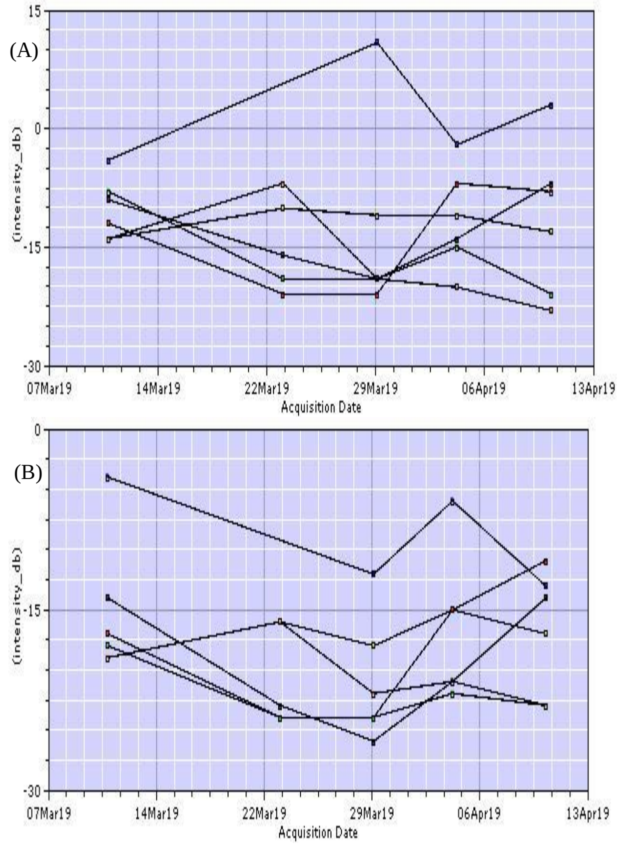

Figure 4. Time Series Pixel Value Reflectance in dB, (A) Reflectance of Pixels in VV band, (B) Reflectance of Pixels in VH band

According to Fig. 4:

it shows that on March11,2019, which is before the flood started, the amount of reflections in the two VV and VH bands is higher than the other dates, indicating that on this day the whole city of Aq'qala is dry and non-flooded.

Almost all VV band reflections are in the range above -16 dB because of their higher reflectance intensity. And most of the reflections in the VH band are less than -16 dB because of the lower reflection intensity.

In the VV band of the first day of flood initiation March23,2019, the reflectance value of the pixels is in the range 12-15, with increasing flooded area on March29,2019 this number reaches 20-25 and at the end flooding again decreases same range 12-15.

In the VH band on March23,2019 the range 17-20 of the flood which reaches the peak on April16,2019 range 22-26. as shown in Fig.4 graph, the value of reflectance in VH band is less than the VV band.

4. RESULTS

Due to approaching the spring, the observed rainy day often occurs in a short period. The rainstorm can cause flooding on land that does not have appropriate infiltration. Moreover, the flowing upstream waters from rivers to the downstream areas. About 10 km of Gorganrood river crossing the Aq'qala city, due to the low slope of the Gorganrood river in the Aq'qala city, the flood is slowly flowing in the river. The minimum and maximum and average of river level are respectively 20 meters, 12.6 meters, 15.9 meters, from sea water level. The maximum and average slope of the river is 4% and 1.1% respectively, which makes the slope near the sea to zero and even negative, which causes water refused. time series of flooding in RGB clustering for aq'qala city is shown in Fig.5

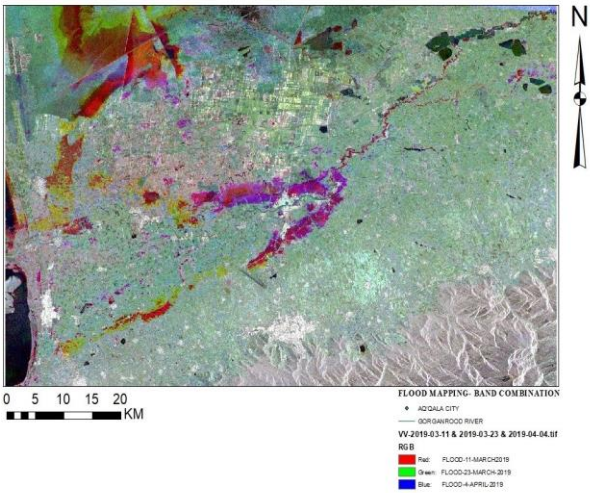

Figure 5. Bands combination in VV channel: Red Band: Flood-11/3/2019, Green Band: Flood-23/3/2019, Blue Band: Flood-4/4/2019

Topographic of Aq'qala city is at a lower level than its surroundings, its surface is flat and its level is lower than free seas. The waters that are entering the city do not have an outlet point and make the city looks like a lake. Therefore, the zoning and identification of areas under flooding are priority for these cities to provide solutions to control and prevent them.

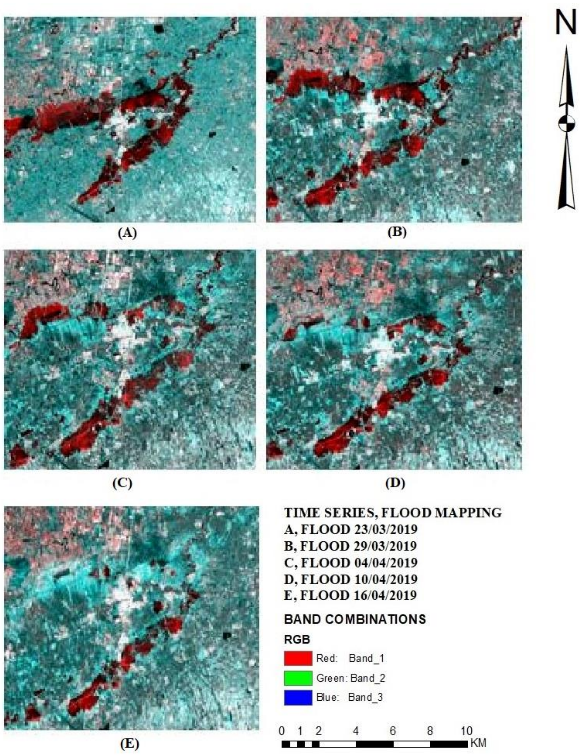

Figure 6. Time series flood mapping of Aq'qala city

As shown in Fig. 6 in peak day, the area which covered by the floodwater on march 23rd were about 96.8 (km^2). In Fig. 6 and Fig. 7 are shown change trend flooded areas.

Date	Area of Flood Mapping (km^2)
11rd March 2019	0
23rd March 2019	96.8
29rd March 2019	53.35
04rd April 2019	33.47
10rd April 2019	25.25
16rd April 2019	11.83

Table 2. Area of Flood Map for time series, Based on initiating of Flood to Mitigation of Flood

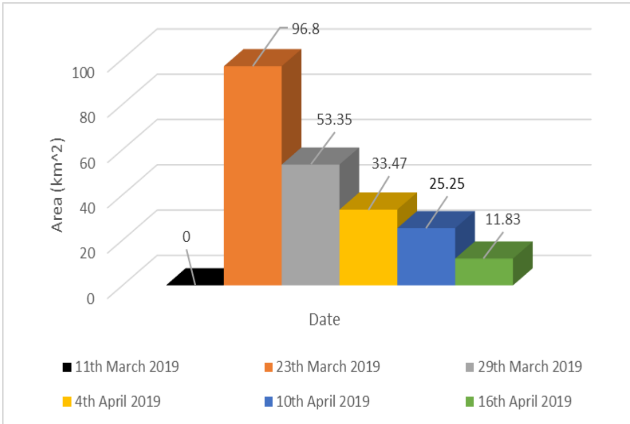

Figure 7. Chart of flood areas changing in Aq'qala city

4.1 Conclusion

One of the most innovative aspects of latest generation sensors is their much increased capacity of acquiring images of the earth surface at regular, short intervals, with respect to previous missions. This constitutes a formidable step forward in the acquisition of data for the study of surface processes (Guyet and Nicolas, 2016a). Also, long time series of detailed remotely sensed maps are very useful in the performance assessment and calibration of hydraulic models. Aq'qala city has always been at risk of flooding because of crossing Gorganrood River, in March 2019 occurred a flood with 50 year return period, the maximum flow rate in Gorganrood was 739 (m^3 /s). Flood maps obtained are very useful for development path of A'qala city, due to the flood maps obtained, some points are important to mention: Passing discharge in Gorganrood river in normal mode is about 100 (m^3 /s), but maximum flow rate in spring was about 739 (m^3 / s). The topography of Aq'qala city is flat due to the flood cannot flowing to outlet. The average slope in Aq'qala city is about 1%. and the average slope in Gorganrood river is about 1.1%. The Gorganrood River at the entrance of the Aq'qala city, due to its lack of land drainage and low latitudes and depths, the flood has covered the surrounding land. According to the zoning maps, first the environment of the Aq'qala city is flooded, then these waters enter the urban environment due to topographic conditions. The first solution to prevent the flow of floodwater into the city, dig up channels around the city for collecting and carrying floodwater to outside the city. At the end, the details of the flood in the VV band were

https://doi.org/10.5194/isprs-archives-XLII-4-W18-415-2019

better than the VH band, so we used the VV band to identify the floods.

ACKNOWLEDGEMENTS

We appreciate to Regional Water Authority and Natural Resources and Watershed Management Organization of Golestan province for some data sharing.

REFERENCES

Amarnath, G., Rajah, A., 2016. An evaluation of flood inundation mapping from MODIS and ALOS satellites for Pakistan. Geomatics, Natural Hazards and Risk 7(5):1526–1537

Betbeder, J., Rapinel, S., Corpetti, T., Pottier, E., Corgne, S Hubert, Moy, L., 2013. Multi-temporal classification of TerraSAR-X data for wetland vegetation mapping. Remote Sensing for Agriculture, Ecosystems, and Hydrology XV 8887:88871B

Chowdhury, EH., Hassan, QK., 2017. Use of remote sensing data in comprehending an extremely unusual flooding event over southwest Bangladesh. Natural Hazards. Springer Netherlands 88(3):1805–1823

Clement, MA., Kilsby, CG., Moore, P., 2017. Multi-Temporal SAR Flood Mapping using Change Detection. Journal of Flood Risk Management 11(2)

De Moel, H., Van Alphen, J., Aerts, JCJH., 2009. Flood maps in Europe - Methods, availability and use. Natural Hazards and Earth System Science 9(2):289–301

Guyet, T., Nicolas, H., 2016. Long term analysis of time series of satellite images. Pattern Recognition Letters. Elsevier B.V. 70:17–23. Available at: http://dx.doi.org/10.1016/j.patrec.2015.11.005

Klemas, V., 2013. Remote sensing of emergent and submerged wetlands: an overview. International Journal of Remote Sensing 34(18):6286–6320

Kumar, G., Parth Sarthi, P., Ranjan, P., Rajesh, R., 2016. Performance of k-means based satellite image clustering in RGB and HSV color space. 2016 International Conference on Recent Trends in Information Technology, ICRTIT 2016 1–5

Manjusree, P., Prasanna Kumar, L., Bhatt, CM., Rao, GS., Bhanumurthy, V., 2012. Optimization of threshold ranges for rapid flood inundation mapping by evaluating backscatter profiles of high incidence angle SAR images. International Journal of Disaster Risk Science 3(2):113–122

Mohamed, INL., Verstraeten, G., 2012. Analyzing dune dynamics at the dune-field scale based on multi-temporal analysis of Landsat-TM images. Remote Sensing of Environment. Elsevier Inc. 119:105–117. Available at: http://dx.doi.org/10.1016/j.rse.2011.12.010

Shen, X., Wang, D., Mao, K., Anagnostou, E., Hong, Y., 2019. Inundation Extent Mapping by Synthetic Aperture Radar: A Review. Remote Sensing 11(7):879

Tsyganskaya, V., Martinis, S., Marzahn, P., Ludwig, R., 2018. Detection of temporary flooded vegetation using Sentinel-1 time series data. Remote Sensing 10(8):1–23

Twele, A., Cao, W., Plank, S., Martinis, S., 2016. Sentinel-1-based flood mapping: a fully automated processing chain. International Journal of Remote Sensing 37(13):2990–3004